Med Biol Eng Comput
DOI 10.1007/s11517-011-0764-9

SPECIAL ISSUE - ORIGINAL ARTICLE

Size matters: MEG empirical and simulation study on source localization of the earliest visual activity in the occipital cortex

Sanja Josef Golubic · Ana Susac · Veljko Grilj · Douglas Ranken · Ralph Huonker · Jens Haueisen · Selma Supek

Received: 10 January 2011 / Accepted: 10 March 2011

Abstract While the relationship between sensory stimulation and tasks and the size of the cortical activations is generally unknown, the visual modality offers a unique possibility of an experimental manipulation of stimulus size-related increases of the spatial extent of cortical activation even during the earliest activity in the retinotopically organized primary visual cortex. We used magnetoencephalography (MEG), visual stimuli of increasing size, and numerical simulations on realistic cortical surfaces to explore the effects of increasing spatial extent of the activated cortical sources on the neuromagnetic fields, location estimation biases, and source resolution. Source localization was performed assuming multiple dipoles in a sphere model using an efficient, automatically restarted multi-start simplex minimizer within the Calibrated Start Spatio-Temporal (CSST) algorithm. We found size-related effects on amplitude and latencies and differences in relative locations of the earliest occipital sources evoked by stimuli of increasing size presented at the same eccentricity. This finding was confirmed by single patch simulations. Additionally, simulations of multiple extended sources demonstrated size-related increase in limits in source resolution for bilaterally simulated sources, biases in location estimates for a given separation of sources, and limits in source resolution due to source multiplicity within a hemisphere.

Keywords Magnetoencephalography (MEG) · Stimulus size · Cortical source extent · Neuromagnetic multi-source localization · Retinotopic organization of the human visual cortex · Cortical magnification factor · Occipital visual cortex

1 Introduction

Magnetoencephalography (MEG) as a real time, direct measure of neuronal activity relies on source modeling assumptions and head model approximations to track dynamic cortical pathways with millisecond temporal resolution. Most of the MEG empirical source localization studies (for a review, see [1]) use single or multiple dipole models which assume one or a small number of focal cortical activations active across time. For distant MEG extracranial measurements, distant compared to the extent of the cortical activation, the dipole approximation has been found to be adequate for realistic generators of human brain activity [8].

There is converging evidence from all functional brain imaging methods that distributed networks of cortical foci underlie sensory and cognitive processes. The spatial extent of each of the cortical activations, however, is largely unknown. Extended cortical activations can be

S. Josef Golubic · A. Susac · S. Supek (✉)
Department of Physics, Faculty of Science, University of Zagreb, Bijenicka c. 32, 10000 Zagreb, Croatia
e-mail: selma@phy.hr

V. Grilj
Rudjer Boskovic Institute, Bijenicka c. 54, 10000 Zagreb, Croatia

D. Ranken
Los Alamos National Laboratory, Los Alamos, NM 87545, USA

R. Huonker · J. Haueisen
Department of Neurology, Friedrich Schiller University, PF 07737 Jena, Germany

J. Haueisen
Department for Biomedical Engineering and Informatics, Technical University Ilmenau, Ehrenbergstrasse 29, 98693 Ilmenau, Germany

Published online: 08 April 2011

expected related to processes of cortical plasticity and late sensory processing [10, 17]. Lü and Williamson [17] reported that coherent neural activity giving rise to long-latency sensory evoked components of event-related magnetic fields (ERFs) and electric potentials (ERPs) extends over cortical areas typically between 40 and 400 mm^2.

Numerical simulations using patches of increasing size (64–256 mm^2) over a realistic cortical surface derived from MRI [11] demonstrated that large patches have a strong net-current moment and are generally more visible to the MEG system, yet less appropriately modeled as single dipoles. For gyral activation, localization bias was about 1 cm, while on the sulcal walls the bias was only on the order of 1 mm. Source estimation methods based on current multipoles were proposed to improve localization estimates for single extended activations over realistic brain surface [7, 14]. Numerical simulations [15] demonstrated that localization accuracy deteriorates for both a classical dipole and a regularized multipole model as the spatial extent of cortical activation increases, while their novel approach outperformed single dipole model by about 1 mm for the largest patches. Current multipole expansion was also used to estimate the lateral source extent [18]. The forward analytic calculations up to octapolar order for a spherical volume conductor and a linear source estimated the lateral extent with negligible bias. Nolte and Curio [18] interpreted the octapole coefficient as the variance of the source distribution which is a valid interpretation only if the source distribution does not change sign. They indicated that with noisy data, the extended nature of the source cannot be seen by this method, and that it cannot be seen by any method if no further assumptions are made relating, for example, the number of activated voxels and their contingency (for fMRI) or amplitude or source strength (for MEG) to the source extent. The later approach is used in all studies aiming at retrieving the spatial extent of cortical activation from non-invasive functional brain imaging measures, e.g., [21–23].

Quantitative evaluation of cortical areas would be relevant for monitoring processes such as developmental plasticity, neural processes mediating learning and reorganization related to training, therapy, disease progression, aging, etc. From a modeling perspective, however, an empirical quantitative insight into spatial extent of cortical activation would be valuable for improving source models and consequently estimation accuracy.

While, in general, the relationship between sensory stimulations or tasks and the size of the activated cortical patches is unknown, the visual modality offers a unique possibility of an experimental manipulation of stimulus size-related increases of the spatial extent of the activation in some of the known retinotopically organized visual areas [2, 12, 24, 28]. The relationship between the activated cortical surface and the size of the stimulus is non-linear and eccentricity dependant due to the cortical magnification factors that differ across retinotopically organized striate and extrastriate areas [12, 24, 25]. The effects of stimulus size have been reported for MEG [16] and ERP responses [20] as well as visual gamma-band responses in human EEG [6]. Functional MRI study [34] demonstrated strong effects of the facial stimulus size both on the fusiform face area and the primary visual area V1.

To our knowledge, there are no studies on empirical evaluations of the localization biases related to the stimulus size increases. The goals of our MEG empirical and simulation studies were to explore stimulus size and eccentricity-related effects on source location estimates and source resolution related to expected increases of the extent of cortical activations. Due to the activation of the multiple retinotopically organized areas during early visual activity [16, 28, 31], the focus of our analysis of empirical data was on the localization of the earliest occipital sources. In addition, numerical simulations using realistic cortical geometry were conducted to estimate biases in location estimates for single focal and extended cortical patches placed at different depths along the calcarine fissure. Limited sets of forward calculations were conducted for multi-source bilateral configurations of two and four focal and extended patches whose separation varied to explore location biases for multi-source configurations together with spatial extent related limits in source resolution.

2 Methods

2.1 Visual study

Six healthy female subjects ranging in age from 23 to 35 years participated in the study. The study was approved by the Ethics Committee of the University in Jena. All subjects gave informed consent before taking part in the experiment.

Visual stimulation was performed using two cycles black and white circular sinusoids, target stimuli, of increasing diameters of 0.3°, 0.9°, and 2°, respectively (Fig. 1). Spatial contrast of the stimuli was 75%. Targets were presented one at a time, in random order, at the center of the visual field (CVF) or at a foveal location (3° right to the vertical meridian and 3° below the horizontal meridian) in the lower right visual field (LRVF) with a duration of 300 ms. Stimulus presentation rate was 1 Hz with an ISI (interstimulus interval) jitter rate of 500 ms. Visual stimulation was controlled by the Presentation software (Neurobehavioral Systems Inc., Albany, CA) and run on a personal computer. The stimuli were randomly repeated until 100 evoked responses were online averaged for each of the six conditions.

Magnetic fields were recorded in a magnetically shielded room at the Biomagnetic Center, Friedrich Schiller University Jena, Germany using a 306-channel MEG system (Elekta Neuromag Oy, Helsinki, Finland). The neuromagnetic activity was continuously recorded with a sampling rate of 1 kHz and bandwidth from 0 to 100 Hz. For artifact elimination, EOG signals were simultaneously recorded with the MEG signals. For each subject, anatomical 3D volumetric T1-weighted magnetic resonance images were obtained from a Siemens Magnetom Vision 1.5T scanner. The Spatiotemporal Signal Space Separation method (tSSS) [29, 30] was used to remove external interference from the data. All data were preprocessed using MEGAN, an MEG data visualization and analysis tool developed by Elaine Best, in the Biophysics group, Los Alamos National Laboratory. To extract physiologically relevant activations for this type of study, the MEG data were low-pass-filtered at 40 Hz.

2.2 Source localization

Spatio-temporal source localization was conducted assuming multiple dipoles in a sphere model both for empirical and simulated data. The cortical surface was derived from MRI using an automated segmentation tool and used to estimate the best-fitting sphere for the head model. The time interval of 60–100 ms poststimulus was analyzed for all conditions. Spatio-temporal source analyses of empirical and simulation data were conducted using the Calibrated Start Spatio-Temporal (CSST) program [19] within MRIVIEW, which uses the automated multi-start downhill simplex method for estimating best-fitting source location, strength, and orientation [3, 13]. In CSST, thousands of starting points are selected randomly from the segmented cortical surface and a selected number of neighboring voxels throughout the brain. In our calculations, 6000 starting points were used for empirical and 1500 for simulated data. Data from all sensor locations were used in the spatio-temporal fits using a rotating dipole model. The minimum number of dipoles was estimated using singular value decomposition (SVD) of the selected spatio-temporal data matrix, while the adequate model was selected based on the reduced chi-square measure of goodness-of-fit [26, 27]. Anatomical locations of the sources were determined by reconciling the MEG head-centered coordinate system with participants MRI head-centered coordinate system.

Monte Carlo simulations were used to estimate the effects of the measurement noise on the best-fitting location parameters. We performed 100 Monte Carlo simulations by adding prestimulus based realistic noise estimates determined by the sensor baseline noise variance in the case of empirical data. For simulated forward field estimates, both Gaussian noise with a standard deviation of 20 fT and empirical data based noise estimates were used.

2.3 Simulations

Numerical simulations were conducted using the forward simulator within MRIVIEW. An automatic segmentation procedure was used to segment the cortical surface from the high-resolution MRI data. Subsequently, 3D morphological operations were used to obtain a layer of voxels that approximate the gray/white matter boundary. A smoothed intensity gradient volume, obtained from MRI data, is used to assign orientations to gray/white matter boundary voxels. Patches of the labeled cortical surface were created using morphology and 3D region growing with a spherical constraint. For single and multi-patch source configurations, the actual patch extent depended on the selected start point, the realistic cortical morphology, and the sphere radius. For example, the largest variability in source extent was obtained for S1 and, at one selected start point, the patch surfaces within spheres of increasing radii of 1, 3, and 5 voxels were 7, 122, and 489 mm^2, respectively. For the same sphere radius, depending on the selected start point and the cortical geometry of the two MRIs used the patch surfaces ranged from 1 to 7 mm^2 for the small radius, from 27 to 122 mm^2 from the medium and 108 to 489 mm^2 for the large radius. To create simulated areas of activity, cortical voxels in a region were treated as oriented,

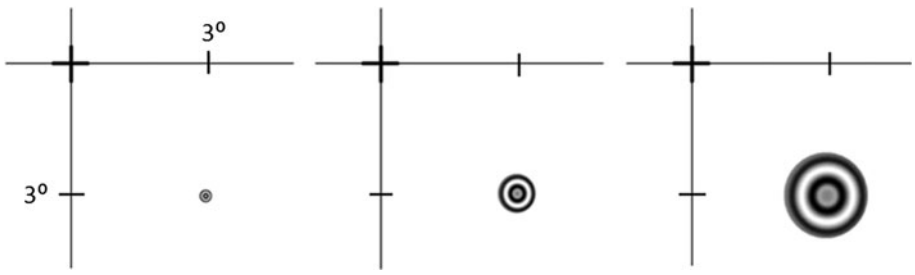

Fig. 1 Circular sinusoids, target stimuli, of increasing size (diameters: 0.3°, 0.9°, and 2°) were presented, one at a time, at two locations: (1) in the lower right visual field (LRVF) 3° bellow the horizontal meridian and 3° right to the vertical meridian and (2) at the fixation point—central visual field (CVF) (not shown)

synchronously active dipoles. Activation time courses were modeled using Gaussians. Maximum current dipole moments were 20, 30, and 40 nAm for small, medium, and large patch sizes, respectively. Forward simulations were conducted assuming Elekta's 306 channel sensor geometry and a spherical head model for cortical patches over a realistic, MRI derived, geometry of two subjects (S1 and S2) that participated in the visual empirical study. Both noiseless and noisy forward calculations were conducted. For noisy simulations, spatially uncorrelated Gaussian noise with standard deviation of 20 fT or empirical data-based noise estimates were added to the calculated field distributions.

Neuromagnetic field distributions were calculated assuming single cortical patches of increasing size located on the same cortical location in the vicinity of the calcarine fissure. Three depths along the calcarine fissure of the two realistic MRI derived cortical surfaces were considered. A series of two-patch synchronously activated configurations were modeled in which patches of increasing size were placed bilaterally and superficially (at a depth of 15 mm) in the vicinity of the calcarine fissure on the two MRI derived realistic cortical surfaces. Four-patch configurations were considered as well in which the separation of the two cortical activations within each hemisphere varied along the calcarine fissure. Source localization was conducted assuming a single dipole model for forward fields generated by single patches. 1- and 2-dipole models were assumed for two-patch configurations. For 4-patch configurations, a model order search was conducted, as it was for the empirical data. For each source location estimate, the distance from the estimated to the given location of the patch start point was calculated as a measure of location bias. In the case of localized synchronous sources, changes in their mutual distance was calculated.

3 Results

3.1 Visual study

The transient neuromagnetic responses to circular sinusoids presented at the fixation point and a foveal location in the LRVF demonstrated size-related effects on latency changes and amplitude modulations. For both centrally and foveally located stimuli, the increasing stimulus size resulted in shorter latencies of the evoked responses. For all stimulus sizes, however, latencies were shorter for the LRVF stimulation compared to the centrally presented stimuli. The averaged transient visually evoked field amplitudes and their spatially integrated root-mean-square values across all magnetometer channels as shown in Fig. 2 for the three subjects correlated with the stimulus size, during the entire interval, regardless of the differences in individual functional cortical geometries. Stimulus size-related amplitude changes were statistically significant for all six subjects and both eccentricities, LRVF ($F(2,15) = 12.21$, $p = 0.00072$) and CVF ($F(2,15) = 27.76$, $p = 9.1E{-}06$).

Figure 3 represents iso-field contour maps of the neuromagnetic field distributions for one subject, at a single latency of 75 ms post-stimulus, evoked by the three circular sinusoids of increasing diameters. Stimulus size increase at both locations in the visual field contributed to amplitude increases. Size-related increased departure from a dipolar pattern is evident when the maps evoked by the smallest stimulus are compared to the maps evoked by the two larger stimuli presented at the same location in the LRVF (right panel). For CVF presentation, departure from a dipolar pattern is prominent only for the largest stimulus (left panel).

Spatio-temporal source localization identified, depending on the condition, 3–5 sources during the earliest measurable evoked responses between 60 and 100 ms. For foveally presented stimuli, the number of the identified sources did not change as a function of the stimulus size. Locations of the occipital sources only, presumably reflecting striate activity, evoked by all three stimuli of increasing size presented in the two locations, the CVF and LRVF, are shown for the same subject in Fig. 4. The extent of the visual stimuli presented centrally affected, however, source resolution. Only for the largest stimulus (green dots) presented in the CVF bilateral occipital sources were identified (Fig. 4b).

Identified earliest occipital source locations for stimuli presented at the same eccentricity, but of different sizes, were different (Fig. 5). The location differences were statistically significant for both eccentricities, LRVF ($F(2,9) = 259.35$, $p = 1.5\text{E}{-}06$) and CVF ($F(2,9) = 83.48$, $p = 4.2E{-}05$). Figure 5a shows a planar projection of the locations for occipital sources evoked by foveally presented stimuli of increasing size in the LRVF for four subjects. Relative spatial distances between the source locations ranged 13–15 mm for S1, 3–9 mm for S2, 8–9 mm for S3, and 7–13 mm for S4. Larger source separations were found for the CVF stimulation (not shown) and were 11–20 mm (34 mm between the bilateral occipital sources evoked the large stimulus) for S1, 15–27 mm for S2, 14–26 mm for S3, and 14–29 mm for S4. In Fig. 5b, differences in the source distances from the head origin are shown across subjects and stimulus sizes.

For all subjects, deeper occipital sources were localized for the smallest stimulus compared to the sources localized for more extended stimuli. Intersubject variability, for example, between the source separations from the smallest and the largest stimuli was evident and ranged 7–13 mm for LRVF (Fig. 5) and 12–15 mm for CVF (not shown). Monte Carlo simulations (not shown), however, confirmed for each condition that realistic measurement noise would result in localization scatter of only about 1 mm. The 10 best-fitting

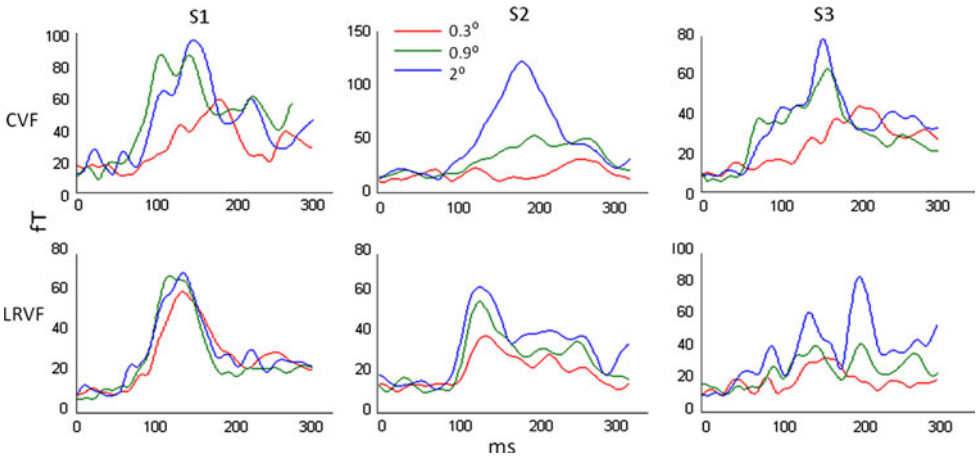

Fig. 2 Root-mean-square value of the evoked neuromagnetic transient responses across all MEG magnetometer channels for the three sizes of stimuli presented at the fixation point (CVF) (upper row) and the location in the LRVF for three subjects

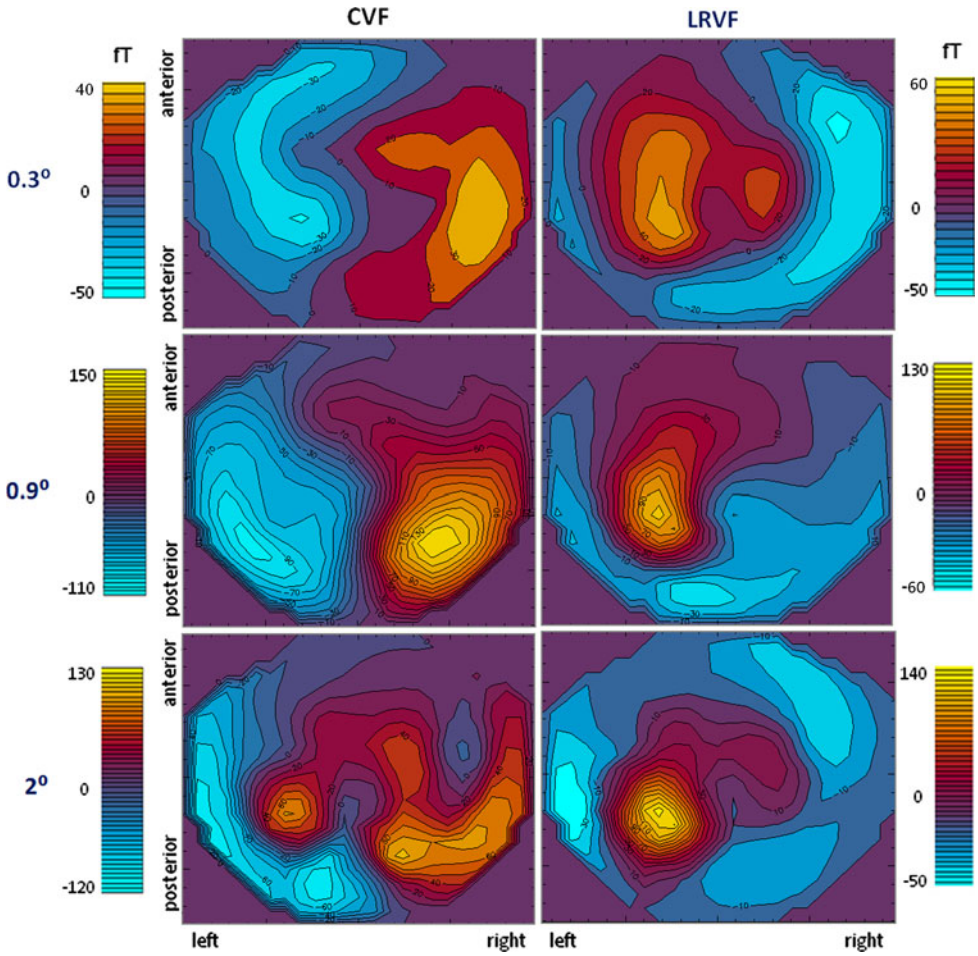

Fig. 3 Iso-field color-coded maps of the neuromagnetic responses at 75 ms post-stimulus evoked by the target stimuli with diameters of 0.3°, 0.9°, and 2° presented in the CVF (*left column*) and a foveal location in the LRVF (*right column*). The color-coded scales are different for each map. The *black iso-field lines* were constructed by interpolation from amplitudes measured relative to pre-stimulus baseline at all magnetometers locations at the selected latency

solution estimates in Fig. 4 which are almost superimposed are indicative of a small scatter of the location estimates.

3.2 Numerical simulations

The CSST source localization using a single dipole model for series of single patch simulated data demonstrated that the error in localization increased with depth and spatial extent of the simulated patch. Depth localization error, however, was less than 1 mm in all noiseless cases and less than 2 mm for all noisy simulations for both realistic head geometries (Table 1).

A series of two-patch configurations were simulated in which patches of increasing size were placed bilaterally

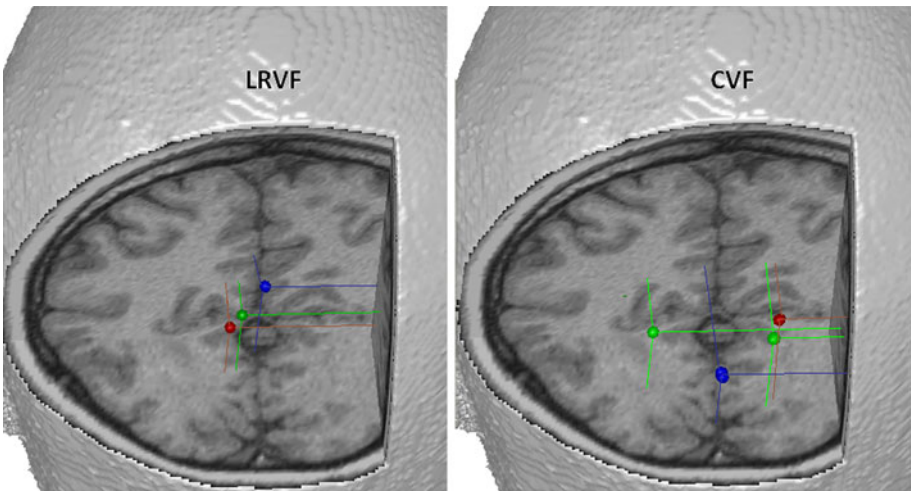

Fig. 4 The best-fitting occipital sources estimated in the 60–100 ms time interval evoked by stimuli of increasing diameter presented in the LRVF (*left panel*) and at the fixation point (*right panel*) are shown for subject S1. In both panels, *red dot* corresponds to source location evoked by the small (0.3°) stimulus, *blue* by the medium (0.9°) and *green* dot(s) by the large (2°) Target stimulus. For each source, 10 best-fitting location estimates are displayed

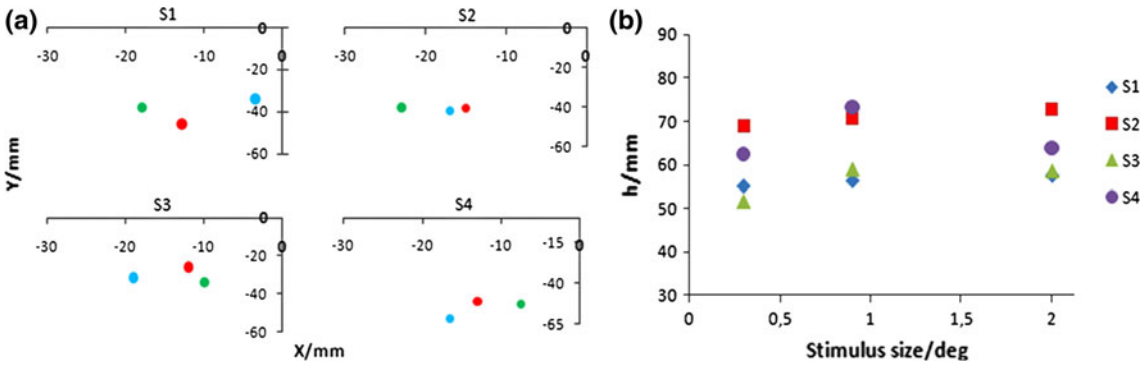

Fig. 5 Panel **a** shows planar projections of the estimated earliest occipital sources for four subjects. The occipital sources were evoked by the target stimuli of increasing diameter (i.e., 0.3°, 0.9°, and 2°) presented at the foveal location in the LRVF. *Red dot* corresponds to source location evoked by the small (0.3°) stimulus, *blue* by the medium (0.9°), and *green* dot(s) by the large (2°) Target stimulus. The diameter of the location dots is proportional to the z-coordinate. Panel **b** shows depth differences (distance from the head origin) of the estimated occipital sources across subjects for the three visual stimuli presented in the LRVF. Note that the locations of the identified occipital sources evoked by the largest stimulus for subjects S1 and S3 are almost identical

Table 1 Cortical patch size-related localization errors for noiseless and noisy single source activations at different depths for S1

Distance from the head center (mm)	Localization error (mm)					
	Focal source (7 mm^2)		Small patch (122 mm^2)		Large patch (489 mm^2)	
78.5	Noiseless	Noisy	Noiseless	Noisy	Noiseless	Noisy
	0.05 ± 0.01	0.10 ± 0.01	0.15 ± 0.01	0.36 ± 0.04	0.17 ± 0.02	0.79 ± 0.08
Distance from the head center (mm)	Localization error (mm)					
	Focal source (1 mm^2)		Small patch (61 mm^2)		Large patch (348 mm^2)	
57.4	Noiseless	Noisy	Noiseless	Noisy	Noiseless	Noisy
	0.21 ± 0.02	0.52 ± 0.07	0.32 ± 0.02	1.30 ± 0.10	0.90 ± 0.20	2.10 ± 0.20

and superficially in the vicinity of the calcarine fissure on the two MRI-derived realistic cortical surfaces. Figure 6 shows iso-field contour maps generated by two focal and extended cortical patches separated 5, 9, and 15 mm.

A dipolar pattern is evident for two focal patches. Increases in separation resulted in amplitude increase and rotation of field extrema. For extended sources, an increase in separation contributed to a decrease in amplitudes and a significant departure from a dipolar pattern (right column of the Fig. 6).

One- and two-dipole models were fitted to the series of two-patch configurations. Independent of the patch size,

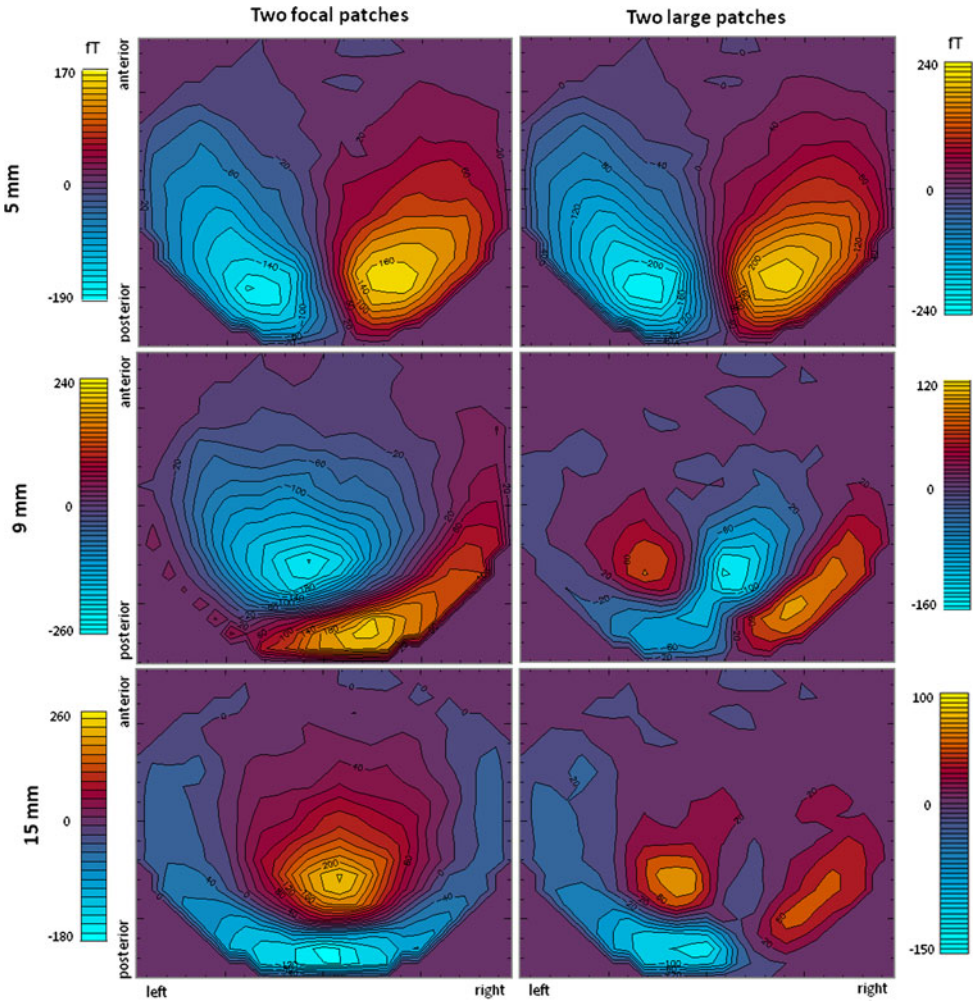

Fig. 6 Iso-field color-coded maps of the simulated neuromagnetic distributions generated by 2 focal (*left column*) and 2 large cortical patches (*right column*) separated 5, 9, and 15 mm. Gaussian noise was added with a standard deviation of 20 fT. The patches of surface areas of 7 and 489 mm^2 were positioned in the two hemispheres in the vicinity of the calcarine fissure at superficial locations 15 mm from the head surface. The color-coded scales, different for each condition, are indicated to the left or to the right of each map. The *black iso-field lines* were constructed by interpolation from the simulated amplitudes at all magnetometers locations at the peak of the assumed Gaussian profile of the simulated patch activity with a total dipole moment of 20 and 40 nAm for the small and large patches, respectively. These maps represent orthogonal surface projections on a plane. Magnitude of positive fields (flux emerging from the head) are displayed in *yellow* range and negative in *blue* range colors

Table 2 Localization error for two-patch configurations for S1 expressed as a departure from the two given distances of the patches of increasing sizes

Actual source distance (mm)	Source area (mm^2)	Estimated distance increase (mm)
9	7	Sources not resolved
	113	1.3 ± 0.2
	489	6.0 ± 0.9
15	7	0.5 ± 0.1
	114	0.8 ± 0.3
	476	1.2 ± 0.3

the two sources were not resolved at a separation of 5 mm. An increase in the simulated cortical patch size contributed to source resolution already at a distance of only 9 mm for the two largest sources. For that configuration, a reduced χ^2 of 1.54 was obtained for a 1-dipole model compared to 1.02 for a 2-dipole model. For larger separations (i.e., 15 mm), the two cortical sources were identified for all patch sizes, however, with a larger localization error for larger patches (Table 2). While the localization error resulted in estimated distance departure of 6 mm for the largest activation patches separated 9 mm it dropped to close to 1 mm only for separation of 15 mm for the same patch sizes. A limited set of four activated patches, two per hemisphere, and the choice of source distances of 5, 9, and 15 mm within hemisphere, all resulted in the identification of no more than a single source per hemisphere (not shown).

4 Discussion

Visual stimuli of increasing size were used in previous studies, e.g. [2, 28] to account for the cortical magnification factor for stimuli placed at peripheral locations in the visual field. In this study, however, circular sinusoids of increasing diameters were placed at the same eccentricity to explore stimulus size-related effects of the expected increases in the spatial extent of cortical activations on source location biases and cortical extent related source discrimination. The two selected eccentricities, central and a foveal in the LRVF

were selected for their most prominent effects on the cortical extent in all retinotopically organized areas [12, 24, 25]. For centrally presented visual stimuli, the estimated [12, 25] spatial extent of the V1 surface was 35 mm^2 for small visual stimulus (0.3°), 262 mm^2 for the medium (0.9°), and 697 mm^2 for the large stimulus (2°). Foveal presentation of the same stimuli resulted in smaller spatial extents in the V1 which were 3, 26, and 129 mm^2 for 0.3°, 0.9°, and 2.0°, respectively. While Lü and Williamson [17] suggested that late sensory processing can activate larger cortical areas up to 400 mm^2, this study demonstrated that extended activation ranging up to 700 mm^2 can be activated also during earliest visual activity. In our simulations, the spatial extent of activated cortical patches was from 1 to more than 500 mm^2 and was larger compared to earlier simulation studies [11, 15].

An increase in the visual stimulus size (Fig. 1) strongly affected evoked neuromagnetic responses during the entire evoked response for all subjects (Figs. 2, 3) in agreement with MEG [16], EEG [6], and ERP [20] studies. Size-related effects on the evoked amplitudes from this study are in agreement also with the latest fMRI study on the strong effects of the lower-level stimulus features such as size, position, and contrast on both V1 and fusiform face area (FFA) responses [34]. Numerical simulations using single cortical patches of increasing spatial extent at each of the three locations along the calcarine fissure confirmed the finding, in agreement with the previous simulation study [11].

Single patch simulations demonstrated that fitting a focal source model to simulated field distributions generated by single cortical patches of increasing extent resulted in location biases of only up to 2 mm for all conditions considered (Table 1). In empirical visual studies, different locations were identified for each stimulus size presented at the same location. While in simulations we were able to evaluate differences between estimated and known patch locations, only relative source separations were evaluated for empirical source location estimates. Size-related differences in relative source locations ranged from few to up to 15 mm, across conditions and subjects for a foveal presentation in the LRVF (Fig. 5). Such findings are in agreement with single patch simulation study on location biases on realistic cortical surfaces [11]. Central visual stimulation resulted in bilateral activation and larger relative separation of the earliest occipital sources ranging from 11 to 29 mm and even 34 mm between the bilateral occipital sources evoked the large stimulus. Bilaterally placed series of two-patch configurations modeling hemifield stimulation reproduced the empirical finding of the identification of two occipital sources only for the largest stimulus size (Fig. 4). Our simulations of two and four extended source configurations (Table 2) are the first multi-source simulations that demonstrated: size-related changes in source resolution for bilaterally simulated sources (Table 2); size-related biases in location estimates for a given separation of bilateral sources; and limits in source resolution due to source multiplicity within a hemisphere.

In empirical visual studies, in particular during later latencies, the location biases can be linked to several factors such as noise, source assumptions related to the cortical extent, source multiplicity, source proximity, and volume approximation. In this study, the analysis period was selected to emphasize, if not isolate, the role of cortical extent of the most dominant occipital source. The noise contribution to location biases was up to 1 mm for all conditions as demonstrated by Monte Carlo simulations, while the spherical volume approximation in the occipital region is expected to result in negligible location biases [9]. Compared to depth and volume conductor biases, in particular in some brain regions, the size-related biases may be smaller [18]. Currently, there are no methods to account efficiently for cortical extent other than the use of source estimation methods based on current multipoles which demonstrated improvement in source localization accuracy of extended patches up to 256 mm^2, however, only for about 1 mm [15] compared to single dipole fitting. It is important to note that multipole expansion is adequate only for reasonably focal activity. Linear approaches, on the other hand, do not include explicit source-size-related assumptions since they assume uniform distribution of thousands of point-current dipoles over a selected surface or volume. Different reconstruction algorithms proposed for such an under-determined problem use mathematical criteria such as lp norm to select a unique solution. They all lead, however, to biases in source location estimates, poor spatial resolution and increasing smearing, i.e., overestimation of activation extent [5]. To avoid under-determination of the linear approaches, Yetik and colleagues proposed a number of spatially distributed line- and surface-source models [32, 33] using a much smaller number of parameters that define the spatial distribution of a single extended source on a 2D surface. Compared to the methods based on multipolar expansion, their models offer added flexibility of the source shape and extent along different directions in 2D, whereas the disadvantage is the increased number of parameters restricting the estimation performance. In addition, it was noted that a priori knowledge about the spatial characteristics of the extended source, which is not available in the empirical studies, is helpful in determining the number and type of the basis functions in their distributed line- and surface-source models as an inappropriate choice of basis functions may result in a poorer fit compared to the focal source model.

Inter-subject variability was evident in our empirical data (Figs. 2, 3) and source estimates (Fig. 5), and was also reproduced via numerical simulations (not shown). Inter-

subject variability has been explored particularly extensively for the primary visual area V1. Anatomical [12], cytoarchitechtonic [4] and functional brain imaging studies using fMRI [22] demonstrated high individual variability in size and shape of V1, and in the relationship to the free surface and sulci. In addition, the positions of areas 17 and 18 were found to differ between the hemispheres [4]. Differences in sizes, shapes, and asymmetries of V1 across hemispheres contribute to large variability in transient responses and ability to localize underlying activity in agreement with this and earlier numerical simulations [11]. Strong inter-subject variability in visual cortex has been reported in earlier MEG studies for striate [2] and extrastriate areas [28] advocating for within subject as opposed to across subjects analysis. It is important to note that MEG reflects primarily activity of primary current sources and consequently reflects differences in the functional neuroanatomy more than ERP. However, most recent study on visually evoked electrical potentials demonstrated large intersubject variability to stimuli of increasing size at a selected contrast level [20] in agreement with our findings.

While the size of a visual stimulus and consequently the size of the activated visual cortex matter in the visual modality and affected the measured responses and estimated location parameters as presented in this study, determining the size of the cortical activation directly from any of the functional brain imaging measures is not easily accomplished. Size retrieval requires further assumptions all of which are likely to lead to under- or over-estimation of spatial cortical extent. While voxel size, voxel contingency, in addition to threshold and temporal integration, contributes to limitations in retrieving the size from the fMRI data, it is the sensitivity of MEG signals to depth and complex cortical morphology, as well as source modeling assumptions and approaches used in source localization that lead to under- or over estimations of cortical extent.

Larger cortical spatial extent can be advantageous by giving rise to stronger signals and, under some circumstances, contributing to source separation, as demonstrated by our simulations. Further studies are needed to explore location and temporal dynamics biases in particular for multiple extended sources such as those that are most likely present during later visual activity evoked by large centrally presented visual stimuli. Studies on spatio-temporal source resolution of extended cortical activations are important for optimizing experimental paradigm designs aiming to explore cognitive processes and the accurate identification of their neuronal basis.

Acknowledgments This study was supported by the Croatian Ministry of Science, Education, and Sport (grant 199-1081870-1252) and bilateral agreement between the University of Zagreb and Technical University of Ilmenau.

References

1. Aine CJ (2010) Highlights of 40 years of SQUID-based brain research and clinical applications. In: Supek S, Susac A (eds) IFMBE proceedings 17th international conference on biomagnetism advances in biomagnetism—Biomag 2010, vol 28. Springer, Heidelberg, pp 9–34
2. Aine CJ, Supek S, George JS, Ranken D, Lewine J, Sanders J, Best E, Tiee W, Wood CC (1996) Retinotopic organization of human visual cortex: departures from the classical model. Cereb Cortex 6:354–361
3. Aine C, Huang M, Stephen J, Christner R (2000) Multistart algorithms for MEG empirical data analysis reliably characterize locations and time courses of multiple sources. Neuroimage 12:159–172
4. Amunts K, Malikovic A, Mohlberg H, Schormann T, Zilles K (2000) Brodmann's areas 17 and 18 brought into stereotaxic space—where and how variable? Neuroimage 11:66–84
5. Baillet S, Mosher JC, Leahy RM (2001) Electromagnetic brain mapping. IEEE Signal Process Mag 18:14–30
6. Busch NA, Debener S, Kranczioch C, Engel AK, Herrmann CS (2004) Size matters: effects of stimulus size, duration and eccentricity on the visual gamma-band response. Clin Neurophysiol 115:1810–1820
7. David O, Garnero L (2002) Time-coherent expansion of MEG/EEG cortical source. Neuroimage 17:1277–1289
8. de Munck JC, van Dijk BW, Spekreijse H (1988) Mathematical dipoles are adequate to describe realistic generators of human brain activity. IEEE Trans Biomed Eng 35:960–966
9. Hämäläinen MS, Sarvas J (1989) Realistic conductivity geometry model of the human head for interpretation of neuromagnetic data. IEEE Trans Biomed Eng 36:165–171
10. Hämäläinen M, Hari R, Ilmoniemi RJ, Knuutila J, Lounasmaa OV (1993) Magnetoencephalography—theory, instrumentation, and applications to noninvasive studies of the working human brain. Rev Mod Phys 65:413–497
11. Hillebrand A, Barnes GR (2002) A quantitative assessment of the sensitivity of whole-head MEG to activity in the adult human cortex. Neuroimage 16:638–650
12. Horton JC, Hoyt WF (1991) Quadratic visual field defects. Brain 114:1703–1718
13. Huang M, Aine CJ, Supek S, Best E, Ranken D, Flynn ER (1998) Multi-start downhill simplex method for spatio-temporal source localization in magnetoencephalography. Electroencephalogr Clin Neurophysiol 108:32–44
14. Jerbi K, Baillet S, Mosher JC, Nolte G, Garnero L, Leahy RM (2002) Modeling realistic patches of cortical activity with current multipoles. Neuroimage 16:638–650
15. Jerbi K, Baillet S, Mosher JC, Nolte G, Garnero L, Leahy RM (2004) Localization of realistic cortical activity in MEG using current multipoles. Neuroimage 22:779–793
16. Laskaris NA, Liu LC, Ioannides AA (2003) Single-trial variability in early visual neuromagnetic responses: an explorative study based on the regional activation contributing to the N70m peak. Neuroimage 20:765–783
17. Lü ZL, Williamson SJ (1991) Spatial extent of coherent sensory-evoked brain activity. Exp Brain Res 84:411–416
18. Nolte G, Curio G (2000) Current multipole expansion to estimate lateral extent of neuronal activity: a theoretical analysis. IEEE Trans Biomed Eng 47:1347–1355
19. Ranken DM, Best ED, Stephen JM, Schmidt DM, George JS, Wood CC, Huang M (2002) MEG/EEG forward and inverse modeling using MRIVIEW. In: Nowak H, Haueisen J, Giebler F, Huonker R (eds) Biomag 2002. Proceedings of the 13th

international conference on biomagnetism. VDE Verlag, Berlin, pp 785–787
20. Ribeiro MJ, Castelo-Branco M (2010) Psychophysical channels and ERP population responses in human visual cortex: area summation across chromatic and achromatic pathways. Vision Res 50:1283–1291
21. Roberts TP, Disbrow EA, Roberts HC, Rowley HA (2000) Quantification and reproducibility of tracking cortical extent of activation by use of functional MR imaging and magnetoencephalography. AJNR Am J Neuroradiol 21:1377–1387
22. Rombouts SA, Barkhof F, Hoogenraad FG, Sprenger M, Valk J, Scheltens P (1997) Test-retest analysis with functional MR of the activated area in the human visual cortex. AJNR Am J Neuroradiol 18:1317–1322
23. Schneider P, Scherg M, Dosch HG, Specht HJ, Gutschalk A, Rupp A (2002) Morphology of Heschl's gyrus reflects enhanced activation in the auditory cortex of musicians. Nat Neurosci 5:688–694
24. Sereno MI, Dale AM, Reppas JB, Kwong KK, Belliveau JW, Brady TJ, Rosen BR, Tootell RB (1995) Borders of multiple visual areas in humans revealed by functional magnetic resonance imaging. Science 268:889–893
25. Slotnick SD, Klein SA, Carney T, Sutter EE (2001) Electrophysiological estimate of human cortical magnification. Clin Neurophysiol 112:1349–1356
26. Supek S, Aine CJ (1993) Simulation studies of multiple dipole neuromagnetic source localization: model order and limits of source resolution. IEEE Trans Biomed Eng 40:529–540
27. Supek S, Aine CJ (1997) Spatio-temporal modeling of neuromagnetic data: I. Multi-source location versus time-course estimation accuracy. Hum Brain Mapp 5:139–153
28. Supek S, Aine CJ, Ranken D, Best E, Flynn ER, Wood CC (1999) Single vs. paired visual stimulation: superposition of early neuromagnetic responses and retinotopy in extrastriate cortex in humans. Brain Res 830:43–55
29. Taulu S, Kajola M (2005) Presentation of electromagnetic multichannel data: the signal space separation method. J Appl Phys 97:124905-1–124905-10
30. Taulu S, Simola J (2006) Spatiotemporal signal space separation method for rejecting nearby interference in MEG measurements. Phys Med Biol 51:1759–1768
31. Vanni S, Tanskanen T, Seppa M, Uutela K, Hari R (2001) Coinciding early activation of the human primary visual cortex and anteromedial cuneus. Proc Natl Acad Sci USA 98:2776–2780
32. Yetik IS, Nehorai A, Muravchik CH, Haueisen J (2005) Line-source modeling and estimation with magnetoencephalography. IEEE Trans Biomed Eng 52:839–851
33. Yetik IS, Nehorai A, Muravchik CH, Haueisen J, Eiselt M (2006) Surface-source modeling and estimation using biomagnetic measurements. IEEE Trans Biomed Eng 53:1872–1882
34. Yue X, Cassidy BS, Devaney KJ, Holt DJ, Tootell RB (2011) Lower-level stimulus features strongly influence responses in the fusiform face area. Cereb Cortex 21:35–47